NASA Technical Paper 3640

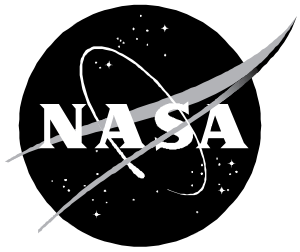

Electromagnetic Scattering From Arbitrarily Shaped Aperture Backed by Rectangular Cavity Recessed in Infinite Ground Plane

C. R. Cockrell and Fred B. Beck
Langley Research Center • Hampton, Virginia

National Aeronautics and Space Administration
Langley Research Center • Hampton, Virginia 23681-0001

May 1997

Acknowledgments

We thank M. D. Deshpande for his many helpful discussions and assistance in the preparation of this paper.

Available electronically at the following URL address: http://techreports.larc.nasa.gov/ltrs/ltrs.html

Printed copies available from the following:

NASA Center for AeroSpace Information
800 Elkridge Landing Road
Linthicum Heights, MD 21090-2934
(301) 621-0390

National Technical Information Service (NTIS)
5285 Port Royal Road
Springfield, VA 22161-2171
(703) 487-4650

Contents

Symbols

$A^+,\ A^-$	areas of D_n^+ and D_n^- triangles
a,b,c	x-, y-, and z-dimensions of rectangular cavity
a_p	complex modal amplitude of pth forward traveling mode
$\mathbf{B}_n(\boldsymbol{r}')$	vector basis function for triangular subdomain
b_p	complex modal amplitude of pth backward traveling mode
D_n^+, D_n^-	two triangles associated with nth common edge
$\mathbf{E}_i$	incident electric field vector
$\mathbf{E}_R$	reflected electric field
$\mathbf{E}_s(2\mathbf{m})$	scattered electric field vector due to **m**
$\mathbf{E}_{s_\theta}, \mathbf{E}_{s_\phi}$	θ and ϕ components of scattered electric far field
$\mathbf{E}_w$	transverse electric field vector inside cavity
$E_{x_i}, E_{y_i}, E_{z_i}$	x-, y-, and z-components of incident electric field
E_{θ_i}, E_{ϕ_i}	θ and ϕ components of incident electric field
EM	electromagnetic
$\mathbf{e}_p, \mathbf{h}_p$	rectangular waveguide vector modal functions for pth mode
$\mathbf{F}$	electric vector potential
F_{n_θ}, F_{n_ϕ}	θ and ϕ components of electric vector potential due to $\mathbf{B}_n$
$\mathbf{H}_i$	incident magnetic field
$\mathbf{H}_R$	reflected magnetic field
$\mathbf{H}_s(2\mathbf{m})$	scattered magnetic field vector due to **m**
$\mathbf{H}_w$	transverse magnetic field vector inside cavity
$\mathbf{j}$	electric surface current density
$\mathbf{k}_i$	propagation vector along incidence direction
k_0	free-space wave number
L	length of cavity
l_n	length of nth edge
$\mathbf{m}$	magnetic surface current density
N	total number of triangular elements on aperture
n	integer associated with triangular subdomains
P	number of cavity modes
p	integer, waveguide modal index
RCS	radar cross section
$\mathbf{r}$	position vector of field point
$\mathbf{r}'$	position vector of source point
$\mathbf{r}_1, \mathbf{r}_2$	position vectors of vertices opposite nth edge
S	cavity aperture surface
$V_{n'}$	(n') th element of column matrix [**V**]

x,y,z	Cartesian coordinates
$\hat{x}, \hat{y}, \hat{z}$	unit vector along *X*-, *Y*-, and *Z*-axis, respectively
α_0	angle, deg
[Γ], [**V**]	column matrices
Γ_n	amplitude of electric current normal to *n*th edge
γ_p	propagation constant of *p*th mode of cavity
ε, μ	permittivity and permeability of free space
η_0	free-space impedance
θ_i, ϕ_i	plane wave incident angles, deg
$\hat{\theta}_i, \hat{\phi}_i$	unit vectors
λ_0	free-space wavelength
$\sigma_{\theta\theta}$	H-copolarized radar cross-section pattern
$\sigma_{\theta\phi}, \sigma_{\phi\theta}$	cross-polarized radar cross-section pattern
$\sigma_{\phi\phi}$	E-copolarized radar cross-section pattern
ω	angular frequency

Abstract

The electromagnetic scattering from an arbitrarily shaped aperture backed by a rectangular cavity recessed in an infinite ground plane is analyzed by the integral equation approach. In this approach, the problem is split into two parts: exterior and interior. The electromagnetic fields in the exterior part are obtained from an equivalent magnetic surface current density assumed to be flowing over the aperture and backed by an infinite ground plane. The electromagnetic fields in the interior part are obtained in terms of rectangular cavity modal expansion functions. The modal amplitudes of cavity modes are determined by enforcing the continuity of the electric field across the aperture. The integral equation with the aperture magnetic current density as an unknown is obtained by enforcing the continuity of magnetic fields across the aperture. The integral equation is then solved for the magnetic current density by the method of moments. The electromagnetic scattering properties of an aperture backed by a rectangular cavity are determined from the magnetic current density. Numerical results on the backscatter radar cross-section (RCS) patterns of rectangular apertures backed by rectangular cavities are compared with earlier published results. Also numerical results on the backscatter RCS patterns of a circular aperture backed by a rectangular cavity are presented.

1. Introduction

Electromagnetic (EM) scattering characteristics of metallic cavities are useful in studying radar cross section and electromagnetic penetration properties of objects consisting of these cavities as substructures. A large body of work which treats these cavities has been reported in the literature (e.g., refs. 1 to 12). In references 9 and 10, the problem of determining the RCS of an aperture backed by a cavity recessed in an infinite ground plane has been solved by the equivalence principle and integral equation approach. The integral equation in references 9 and 10 was solved by discretizing the aperture into rectangular or quadrilateral patches for use in the method of moments. However, when the aperture is of irregular shape with sharp corners and bends or loaded with microstrip patches of irregular shape, the discretization scheme used in references 9 and 10 may not be able to model the aperture efficiently. Discretization of an irregular-shaped aperture into triangular subdomains may be preferred over the quadrilateral patches.

The problem of an arbitrarily shaped aperture backed by a rectangular cavity is formulated in terms of an integral equation with the magnetic surface current density in the aperture as an unknown. Discretizing the aperture into triangular subdomains and using the method of moments transformed the integral equation into a matrix equation, which is solved by standard lower or upper (LU) decomposition techniques. From the magnetic surface current density, the scattered far fields from the arbitrarily shaped aperture are determined. The present method is validated by comparing the numerical results obtained by the present formulation with the results available in reference 9.

The formulation of the problem in terms of integral equations using the surface equivalence principle is developed in section 2, numerical results on the RCS of rectangular apertures backed by rectangular cavities are presented and compared with earlier published results in section 3, and the RCS of a circular aperture backed by a rectangular cavity in an infinite ground plane is also presented in section 3.

2. Theory

Consider an aperture backed by a rectangular cavity recessed in an infinite ground plane as shown in figure 1(a). The cavity is assumed to be illuminated by an electromagnetic plane wave. The problem may then be divided into interior and exterior parts as shown in figures 1(b) and 1(c). With the equivalence principle, the fields in the exterior region can be found by replacing the entire ground plane including the aperture with equivalent electric surface current density **j** and the aperture with equivalent magnetic surface current **m** only. However, with the application of image theory, only the magnetic currents are needed to determine the exterior fields. From the boundary condition of continuous electric fields, the tangential electric fields inside are expressed in terms of $-\mathbf{m}$. If $\mathbf{E}_w$ and $\mathbf{H}_w$ are the EM fields due to $-\mathbf{m}$ inside the cavity and $\mathbf{E}_s$ and $\mathbf{H}_s$ are the EM fields due to $\mathbf{m}$ in the exterior region, then using the continuity of tangential magnetic fields across the aperture gives

$$\mathbf{H}_w|_t = \mathbf{H}_s|_t + 2\mathbf{H}_i|_t \qquad \text{(Over aperture)} \tag{1}$$

where $\mathbf{H}_i$ is the incident magnetic field and the subscript t indicates tangential component to the aperture. Equation (1) is solved for the equivalent magnetic surface currents **m**, from which the scattering properties of the cavity are determined. The electromagnetic fields required to solve equation (1) can be obtained by using the procedure described in section 2.1.

2.1. Electromagnetic Field in Interior Part

The transverse electric and magnetic fields in the cylindrical cavity may be obtained by the superposition of incident and reflected fields as

$$\mathbf{E}_w = \sum_{p=0}^{P} [a_p \exp(-j\gamma_p z) + b_p \exp(j\gamma_p z)]\mathbf{e}_p(x,y) \tag{2}$$

$$\mathbf{H}_w = \sum_{p=0}^{P} [a_p \exp(-j\gamma_p z) - b_p \exp(j\gamma_p z)]Y_p\, \mathbf{h}_p(x,y) \tag{3}$$

where a_p and b_p are amplitudes of the forward and backward traveling waves, γ_p is the propagation constant of pth mode, Y_p is the waveguide modal admittance, and $\mathbf{e}_p(x,y)$ and $\mathbf{h}_p(x,y)$ are the waveguide vector modal functions as defined in references 10 and 11. The analysis in this paper is limited to a rectangular cavity cross section in which fields can be expressed in suitable modal expansion functions. Subjecting the transverse electric field at $z = -L$ to zero allows equations (2) and (3) to be written as

$$\mathbf{E}_w = \sum_{p=0}^{P} -2ja_p \exp(j\gamma_p L) \sin\gamma_p(z+L)\, \mathbf{e}_p(x,y) \tag{4}$$

$$\mathbf{H}_w = \sum_{p=0}^{P} 2a_p \exp(j\gamma_p L) \cos\gamma_p(z+L)\, Y_p\, \mathbf{h}_p(x,y) \tag{5}$$

Because at $z = 0$,

$$\mathbf{E}_t|_{z=0} \times (-\hat{z}) = -\mathbf{m}(x,y)$$

equations (4) and (5) may be written as

$$\mathbf{E}_w = \sum_{p=0}^{P} \frac{-\sin \gamma_p(z+L)}{\sin \gamma_p L} \left[\iint_{\text{Aperture}} \mathbf{m}(x',y') \cdot \mathbf{h}_p(x',y')\, dx'\, dy' \right] \mathbf{e}_p \tag{6}$$

$$\mathbf{H}_w = \sum_{p=0}^{P} \frac{-j \cos \gamma_p(z+L)}{\sin \gamma_p L} \left[\iint_{\text{Aperture}} \mathbf{m}(x',y') \cdot \mathbf{h}_p(x',y')\, dx'\, dy' \right] Y_p\, \mathbf{h}_p(x,y) \tag{7}$$

The aperture is now divided into triangular subdomains as shown in figure 2. The triangular discretization shown in figure 2 is arbitrary. The final results will depend upon the average size of the triangular elements. If the average size of subdomain triangles is small, we expect the results to be more accurate. The triangular discretization shown in figure 2 is obtained by using COSMOS/M software. The magnetic surface current density over the aperture may be expressed in terms of triangular basis functions (ref. 13) as

$$\mathbf{m}(x',y',0) = \sum_{n=1}^{N} \Gamma_n\, \mathbf{B}_n(\mathbf{r}') \tag{8}$$

where Γ_n is the amplitude of electric current normal to the nth edge, $\mathbf{B}_n(\mathbf{r}')$ is the vector basis function associated with the nth edge, and N is the number of nonboundary edges on the aperture surface. The expressions for the basis function are given by (ref. 13)

$$\mathbf{B}_n(\mathbf{r}') = \begin{cases} \dfrac{l_n}{2A^+}(\mathbf{r}' - \mathbf{r}_1) & \left(\text{when } \mathbf{r}' \text{ in } D_n^+\right) \\ -\dfrac{l_n}{2A^-}(\mathbf{r}' - \mathbf{r}_2) & \left(\text{when } \mathbf{r}' \text{ in } D_n^-\right) \end{cases} \tag{9}$$

where all parameters in equations (9) are defined and explained in detail in reference 13.

By using equation (8), the transverse electric and magnetic fields from equations (6) and (7) inside the cavity may be written as

$$\mathbf{E}_w = \sum_{n=1}^{N} \Gamma_n \sum_{p=0}^{P} \frac{-\sin \gamma_p(z+L)}{\sin \gamma_p L} \left[\int\int_{D_n} \mathbf{B}_n(x',y') \cdot \mathbf{h}_p(x',y')\, dx'\, dy' \right] \mathbf{e}_p(x,y) \tag{10}$$

$$\mathbf{H}_w = \sum_{n=1}^{N} \Gamma_n \sum_{p=0}^{P} \frac{-j \cos \gamma_p(z+L)}{\sin \gamma_p L} \left[\int\int_{D_n} \mathbf{B}_n(x',y') \cdot \mathbf{h}_p(x',y')\, dx'\, dy' \right] Y_p\, h_p(x,y) \tag{11}$$

2.2. Electromagnetic Field in Exterior Part

In the exterior part, the electromagnetic field consists of (1) the field due to the incident wave and (2) the field scattered by $\mathbf{m}(x,y)$ backed by an infinite ground plane at $z = 0$.

2.2.1. Incident field. With time variation exp $(j\omega t)$ assumed, the incident electric field may be written as

$$\mathbf{E}_i = \left(\hat{\theta}_i E_{\theta_i} + \hat{\phi}_i E_{\phi_i}\right) \exp\,(-j\mathbf{k}_i \cdot \mathbf{r}) \tag{12}$$

where

$$\mathbf{k}_i = -k_0(\hat{x}\,\sin\,\theta_i\,\cos\,\phi_i + \hat{y}\,\sin\,\theta_i\,\sin\,\phi_i + \hat{z}\,\cos\,\theta_i)$$
$$\mathbf{r} = \hat{x}x + \hat{y}y + \hat{z}z$$

$$E_{\theta_i} = |\mathbf{E}_i|\,\cos\,\alpha_0$$
$$E_{\phi_i} = |\mathbf{E}_i|\,\sin\,\alpha_0$$

and k_0 is the free-space wave number. The angle $\alpha_0 = 0$ corresponds to H-polarization and $\alpha_0 = 90°$ corresponds to E-polarization. (See fig. 1.) From equation (12), the Cartesian components of the incident electric field may be written, respectively, as

$$E_{x_i} = E_{\theta_i}\,\cos\,\theta_i\,\cos\,\phi_i - E_{\phi_i}\,\sin\,\phi_i \tag{13}$$

$$E_{y_i} = E_{\theta_i}\,\cos\,\theta_i\,\sin\,\phi_i + E_{\phi_i}\,\cos\,\phi_i \tag{14}$$

$$E_{z_i} = -E_{\theta_i}\,\sin\,\theta_i \tag{15}$$

The corresponding magnetic field components are obtained through

$$\mathbf{H}_i = \frac{1}{k_0\eta_0}\mathbf{k}_i \times \mathbf{E}_i \tag{16}$$

where η_0 is the free-space impedance. The incident field with $E_{\theta_i} \neq 0$ and $E_{\phi_i} = 0$ is called an H-polarized wave; with $E_{\theta_i} = 0$ and $E_{\phi_i} \neq 0$, an E-polarized wave.

2.2.2. Scattered field due to* m*(x,y,0). For determining the scattered fields in the exterior part, the equivalent magnetic current $\mathbf{m}(x,y,0)$ backed by an infinite conducting plane is considered. Considering the image of $\mathbf{m}(\ )$ in the infinite ground plane, the electromagnetic fields for the exterior part may be written in terms of the magnetic vector potentials $\mathbf{F}(\mathbf{m})$ as

$$\mathbf{E}_s(2\mathbf{m}) = -\frac{2}{\varepsilon}\nabla \times \mathbf{F}(\mathbf{m}) \tag{17}$$

$$\mathbf{H}_s(2\mathbf{m}) = -2j\omega\,\mathbf{F}(\mathbf{m}) - \frac{2j}{\omega\mu\varepsilon}\nabla\nabla \cdot \mathbf{F}(\mathbf{m}) \tag{18}$$

$$\mathbf{F}(\mathbf{m}) = \frac{\varepsilon}{4\pi}\iint_S \mathbf{m}(x',y')\,\frac{\exp\,[-jk_0(\mathbf{r}-\mathbf{r}')]}{|\mathbf{r}-\mathbf{r}'|}\,dS \tag{19}$$

where ε and μ are the permittivity and permeability, respectively, of free-space, and $\mathbf{r}$ and $\mathbf{r}'$ are the coordinates of the field and source points, respectively. With equation (8), the scattered electric and magnetic fields may be written as

$$\mathbf{E}_s(2\mathbf{m}) = \sum_{n=1}^{N} \Gamma_n \frac{-2}{\varepsilon} \nabla \times \mathbf{F}(\mathbf{B}_n) \tag{20}$$

$$\mathbf{H}_s(2\mathbf{m}) = \sum_{n=1}^{N} \Gamma_n \left[-2j\omega\, \mathbf{F}(\mathbf{B}_n) - \frac{2j}{\omega\mu\varepsilon} \nabla\nabla \cdot \mathbf{F}(\mathbf{B}_n) \right] \tag{21}$$

where $\mathbf{F}(\mathbf{B}_n)$ is computed from equation (18) with $\mathbf{B}_n$ replacing $\mathbf{m}$. The total EM fields in the exterior region are now obtained by superposition of the scattered and incident fields as

$$\mathbf{E}_t = \mathbf{E}_s(2\mathbf{m}) + \mathbf{E}_i + \mathbf{E}_R \tag{22}$$

$$\mathbf{H}_t = \mathbf{H}_s(2\mathbf{m}) + \mathbf{H}_i + \mathbf{H}_R \tag{23}$$

where $\mathbf{E}_R$ and $\mathbf{H}_R$ are the reflected electric and magnetic field parts of the incident fields due to the infinite ground plane. In the plane of the infinite ground plane, note that $\mathbf{E}_i + \mathbf{E}_R = 0$ and $\mathbf{H}_i + \mathbf{H}_R = 2\mathbf{H}_i$.

Substituting equations (11) and (21) into equation (1), the magnetic field integral equation with $\mathbf{m}$ or Γ_n as an unknown is obtained as

$$\sum_{n=1}^{N} \Gamma_n \sum_{p=0}^{P} \frac{-j \cos \gamma_p L}{\sin \gamma_p L} \left[\iint_{\text{Aperture}} \mathbf{B}_n(x',y') \cdot \mathbf{h}_p(x',y')\, dx'\, dy' \right] Y_p\, \mathbf{h}_p(x,y)$$
$$= \sum_{n=1}^{N} \Gamma_n \left[-2j\omega\, \mathbf{F}(\mathbf{B}_n) - \frac{2j}{\omega\mu\varepsilon} \nabla\nabla \cdot \mathbf{F}(\mathbf{B}_n) \right] + 2\mathbf{H}_i|_t \tag{24}$$

By selecting $\mathbf{B}_{n'}$ with $n' = 1, 2, 3, \ldots, N$ as a testing function, the application of the method of moments to equation (24) yields

$$\sum_{n=1}^{N} \Gamma_n \sum_{p=0}^{P} \frac{-j \cos \gamma_p L}{\sin \gamma_p L} Y_p \iint_{D_n} \mathbf{B}_n x',y' \cdot \mathbf{h}_p(x',y')\, dx'\, dy'$$
$$\times \iint_{D_{n'}} \mathbf{B}_{n'}(x,y) \cdot \mathbf{h}_p(x,y)\, dx\, dy$$
$$= \sum_{n=1}^{N} \Gamma_n \iint_{D_{n'}} \mathbf{B}_{n'}(x,y) \cdot \left[-2j\omega\, \mathbf{F}(\mathbf{B}_n) - \frac{2j}{\omega\mu\varepsilon} \nabla\nabla \cdot \mathbf{F}(\mathbf{B}_n) \right] dS_{n'}$$
$$+ \iint_{D_{n'}} \mathbf{B}_{n'}(x,y) \cdot 2\mathbf{H}_i|_t\, dx\, dy \tag{25}$$

Equation (24) may be written in matrix form as

$$[\mathbf{Y}]\ [\Gamma] = [\mathbf{V}] \tag{26}$$

where the elements of matrix $[\mathbf{Y}]$ are given by

$$Y_{n'n} = \sum_{p=0}^{P} \frac{-j \cos \gamma_p L}{\sin \gamma_p L} Y_p \iint_{D_n} \mathbf{B}_n(x',y') \cdot \mathbf{h}_p(x',y')\, dx'\, dy'$$
$$\times \iint_{D_{n'}} \mathbf{B}_{n'}(x,y) \cdot \mathbf{h}_p(x,y)\, dx\ \ dy$$
$$- \iint_{D_{n'}} \mathbf{B}_{n'} x,y \cdot \left[-2j\omega\, \mathbf{F}\mathbf{B}_n - \frac{2j}{\omega\mu\varepsilon} \nabla\nabla \cdot \mathbf{F}\mathbf{B}_n \right] dS_{n'} \tag{27}$$

and the elements of $[\mathbf{V}]$ are given by

$$V_{n'} = \iint_{D_{n'}} \mathbf{B}_{n'}(x,y) \cdot \mathbf{H}_i|_t\, dx\, dy \tag{28}$$

Equation (26) is used to determine the magnetic current on the aperture. The far field due to **m** is obtained with the procedure in section 2.3.

2.3. Far Field

By using the far-field approximation, the scattered electric far fields in the (θ,ϕ) direction may be obtained from equation (20) as (fig. 1)

$$E_{s_\theta} = -2 \sum_{n=1}^{N} \Gamma_n\, jk_0 F_{n_\phi} \tag{29}$$

$$E_{s_\phi} = 2 \sum_{n=1}^{N} \Gamma_n\, jk_0 F_{n_\theta} \tag{30}$$

where F_{n_θ} and F_{n_ϕ} are given by

$$\mathbf{F}_n = \hat{\theta} F_{n_\theta} + \hat{\phi} F_{n_\phi}$$
$$= \frac{\exp(-jk_0 r)}{4\pi r} \iint_{D_n} \mathbf{B}_n \exp\left[jk_0 \sin\theta (x' \cos\phi + y' \sin\phi) + jk_0 z' \cos\theta \right] dS_n \tag{31}$$

where r is distance to far field. The copolarized radar cross-section pattern of an aperture backed by a cavity in a three-dimensional conducting surface can be obtained from

$$\sigma_{\theta\theta} = \lim_{r\to\infty} 4\pi r^2 \frac{\left|E_{s_\theta}\right|^2}{\left|E_{\theta_i}\right|^2} \tag{32}$$

for H-polarized incidence and

$$\sigma_{\phi\phi} = \lim_{r\to\infty} 4\pi r^2 \frac{\left|E_{s_\phi}\right|^2}{\left|E_{\phi_i}\right|^2} \tag{33}$$

for E-polarized incidence. The cross polarized radar cross-section pattern is obtained by using

$$\sigma_{\phi\theta} = \sigma_{\theta\phi} = \lim_{r\to\infty} 4\pi r^2 \frac{\left|E_{s_\phi}\right|^2}{\left|E_{\theta_i}\right|^2} = \lim_{r\to\infty} 4\pi r^2 \frac{\left|E_{s_\theta}\right|^2}{\left|E_{\phi_i}\right|^2} \tag{34}$$

3. Numerical Results

The RCS of an arbitrarily shaped aperture backed by a cylindrical cavity recessed in an infinite ground plane is determined by solving the matrix equation (26) for $[\Gamma]$. The cylindrical cavity may be of rectangular, circular, or coaxial cross section. In fact, the method is applicable to any regularly shaped cavity in which EM fields can be expressed in the appropriate modal functions. The matrix elements required for the solution of equation (26) are determined from equations (27) and (28) and numerical integration over the triangles. For numerical integration over the triangles, a 13-point Gaussian quadrature formula (ref. 14) is used. Numerical convergence of matrix equation (26) depends upon the choices of values of N and P. For numerical convergence, sufficiently large values of N and P were selected in all the examples considered. For evaluation of the self terms, that is when $n = n'$, closed-form expressions given in reference 15 are used. The magnetic surface current density obtained from the solution of equation (26) is then used in equations (29) and (30).

A rectangular aperture with x and y equal to $0.7\lambda_0$ and $0.1\lambda_0$, respectively, and backed by a rectangular cavity of depth $1.73\lambda_0$ is selected as a first example to validate the present method of moment and modal expansion method. This example is selected because its RCS patterns calculated with other numerical techniques are available in reference 9. The rectangular aperture for the present method was divided into triangular subdomains. The backscatter RCS pattern of the rectangular aperture is computed as a function of the number of triangular subdomains (i.e., N) and number of cavity modes (i.e., P). The results of these computations are presented in figures 3 and 4. The conclusion may be that for convergence of numerical results, the average area of the triangular subdomain must be less than $0.002\lambda^2$ and $P \geq 20$. The cavity modes considered were selected in the ascending order of their cutoff frequencies. For the numerical examples considered in this paper, the authors did not observe any specific pattern of cavity modes that may enhance the convergence. Figure 5 shows backscatter RCS patterns of the rectangular aperture computed with the present method and earlier published results of reference 9. There is good agreement between the two results. Additional backscatter RCS patterns for a long and narrow cavity ($a = 2.5\lambda_0$, $b = 0.25\lambda_0$) with depth equal to $c = 0.25\lambda_0$ computed with the present method are shown in figure 6 along with earlier published results of reference 9.

Figure 7 shows a circular aperture backed by a rectangular cavity recessed in an infinite ground plane and excited by an EM plane wave. The RCS pattern of the circular aperture is calculated by the present method and presented in figure 8.

4. Concluding Remarks

The electromagnetic scattering from a rectangular aperture backed by a rectangular cavity recessed in an infinite ground plane has been analyzed by the integral equation approach. The electromagnetic fields outside the cavity are obtained in terms of the half-space Green's function and the magnetic surface current density flowing over the aperture. The electromagnetic fields inside the cavity are obtained in terms of cavity modal functions. The integral equation with the magnetic surface current density as an unknown variable is derived by enforcing the continuity of the electric and magnetic fields over the aperture. The magnetic current density is determined by solving the integral equation in conjunction with the method of moments. The backscatter patterns of rectangular and circular apertures backed by rectangular cavities are determined from knowledge of the magnetic current.

The numerical results for rectangular apertures backed by rectangular cavities are compared with earlier published results. There is good agreement between the results obtained by the present method and earlier published data. The radar cross section of a circular aperture backed by a rectangular cavity is also presented. Even though numerical results on rectangular and circular apertures backed by rectangular cavities are presented in this report, the present method can be extended to analyze an arbitrarily shaped aperture backed by circular or coaxial cavities.

NASA Langley Research Center
Hampton, VA 23681-0001
December 11, 1996

5. References

1. Senior, T. B. A.: Electromagnetic Field Penetration Into a Cylindrical Cavity. *IEEE Trans. Electromagn. Compat.*, vol. EMC-18, May 1976, pp. 71–73.

2. Mautz, J. R.; and Harrington, R. F.: Electromagnetic Penetration Into a Conducting Circular Cylinder Through a Narrow Slot—TE Case. *J. Electromagn.* Wav*es & Appl.*, vol. 2, no. 3–4, 1988, pp. 269–293.

3. Ziolkowski, Richard W.; and Grant, J. Brian: Scattering From Cavity-Backed Apertures: The Generalized Dual Series Solution of the Concentrically Loaded E-Pol Slit Cylinder Problem. *IEEE Trans. Antennas & Propag.*, vol. AP-35, no. 5, May 1987, pp. 504–528.

4. Jeng, Shyh-Kang: Scattering From a Cavity-Backed Slit in a Ground Plane—TE Case. *IEEE Trans. Antennas & Propag.*, vol. 38, Oct. 1990, pp. 1523–1529.

5. Senior, Thomas B. A.; and Volakis, John L.: Scattering by Gaps and Cracks. *IEEE Trans. Antennas & Propag.*, vol. 37, June 1989, pp. 744–750.

6. Barkeshli, K.; and Volakis, J. L.: Electromagnetic Scattering From an Aperture Formed by a Rectangular Cavity Recessed in a Ground Plane. *J. Electromagn. Waves & Appl.*, vol. 5, no. 7, 1991, pp. 715–734.

7. Lee, Choon S.; and Lee, Shung-Wu: RCS of a Coated Circular Waveguide Terminated by a Perfect Conductor. *IEEE Trans. Antennas & Propag.*, vol. AP-35, Apr. 1987, pp. 391–398.

8. Lee, Shung-Wu; and Ling, Hao: *Data Book for Cavity RCS*. Tech. Rep. SWL89-1, Univ. of Illinois, Jan. 1989.

9. Jin, J. M.; and Volakis, J. L.: A Finite Element-Boundary Integral Formulation for Scattering by Three-Dimensional Cavity-Backed Apertures. *IEEE Trans. Antennas & Propag.*, vol. 39, no. 1, Jan. 1991, pp. 97–104.

10. Wang, T.; Harrington, R. F.; and Mautz, J. R.: Electromagnetic Scattering From and Transmission Through Arbitrary Apertures in Conducting Bodies. *IEEE Trans. Antennas & Propag.*, vol. 38, no. 11, Nov. 1990, pp. 1805–1814.

11. Harrington, Roger F.: *Time-Harmonic Electromagnetic Fields*. McGraw-Hill Book Co., Inc., 1961.

12. Wang, Tai-Mo; and Ling, Hao: Electromagnetic Scattering From Three-Dimensional Cavities Via a Connection Scheme. *IEEE Trans. Antennas & Propag.*, vol. 39, Oct. 1991, pp. 1505–1513.

13. Rao, S. M.; Glisson, A. W.; and Wilton, D. R.: Electromagnetic Scattering by Surfaces of Arbitrary Shape. *IEEE Trans. Antennas & Propag.*, vol. AP-30, May 1982, pp. 409–418.

14. Zienkiewicz, O. C.: *The Finite Element Method in Engineering Science*. McGraw Hill Book Co., Inc., 1971.

15. Wilton, Donald R.; Rao, S. M.; Glisson, Allen W.; Schaubert, Daniel H.; Al-Bundak, O. M.; and Butler, Chalmers M.: Potential Integrals for Uniform and Linear Source Distributions on Polygonal and Polyhedral Domains. *IEEE Trans. Antennas & Propag.*, vol. AP-32, no. 3, Mar. 1984, pp. 276–281.

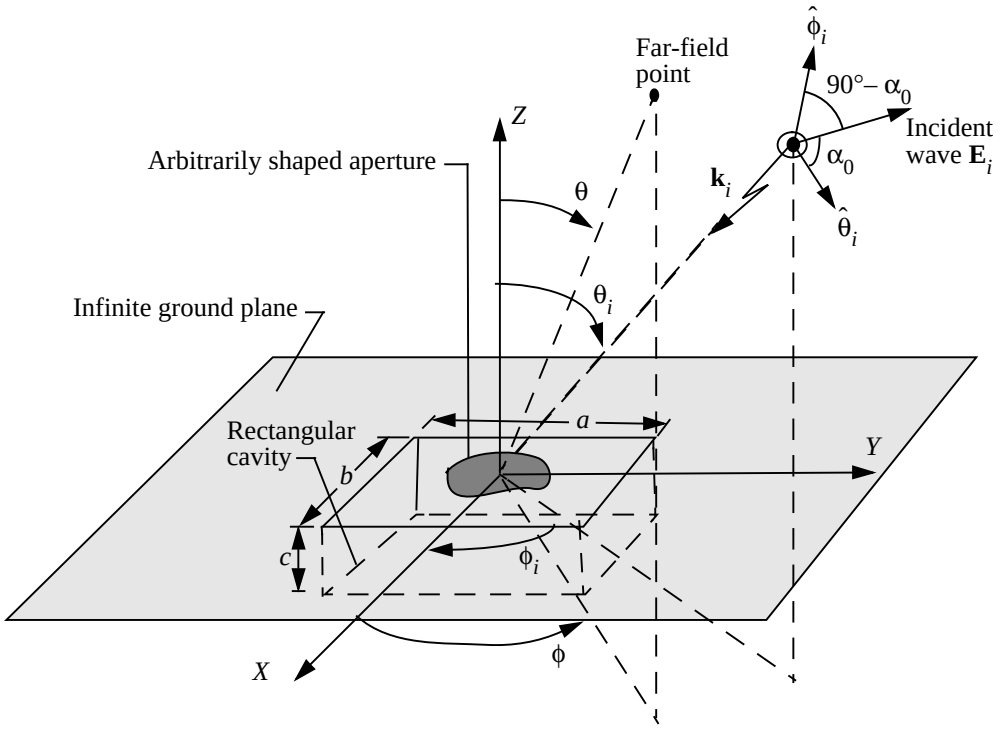

(a) Geometry.

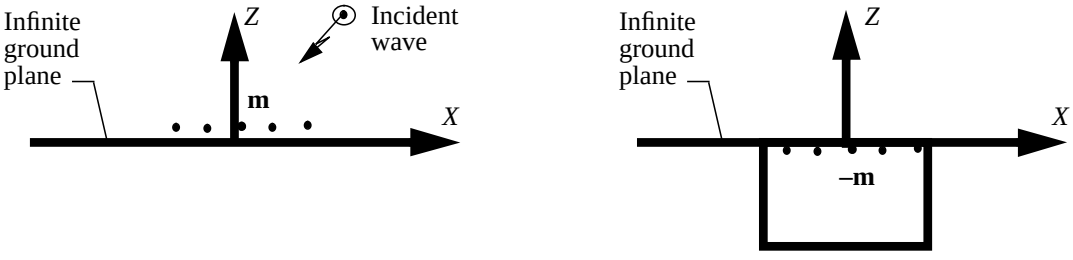

(b) Equivalent exterior problem.

(c) Equivalent interior problem.

Figure 1. Rectangular aperture backed by a rectangular cavity recessed in an infinite ground plane.

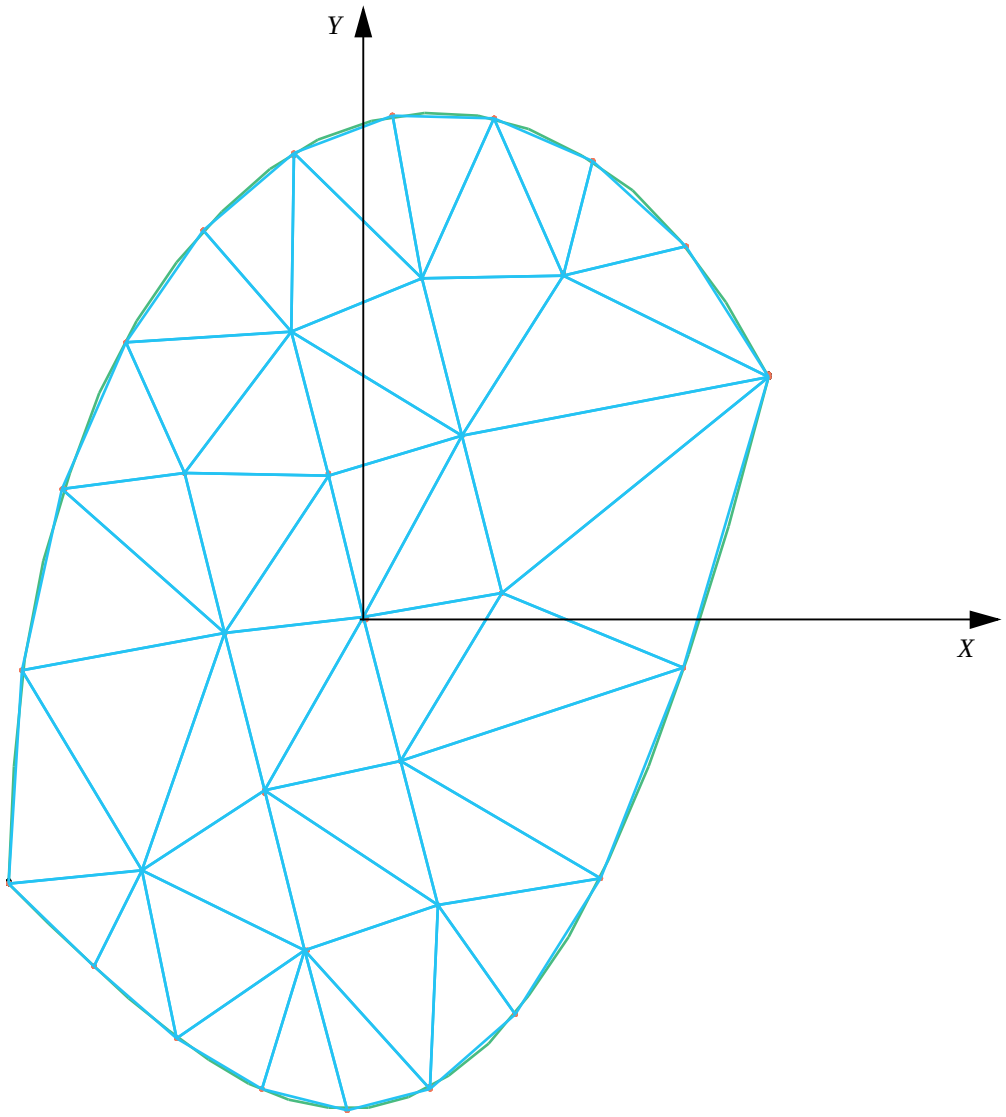

Figure 2. Geometry of arbitrary aperture discretized into triangular subdomains.

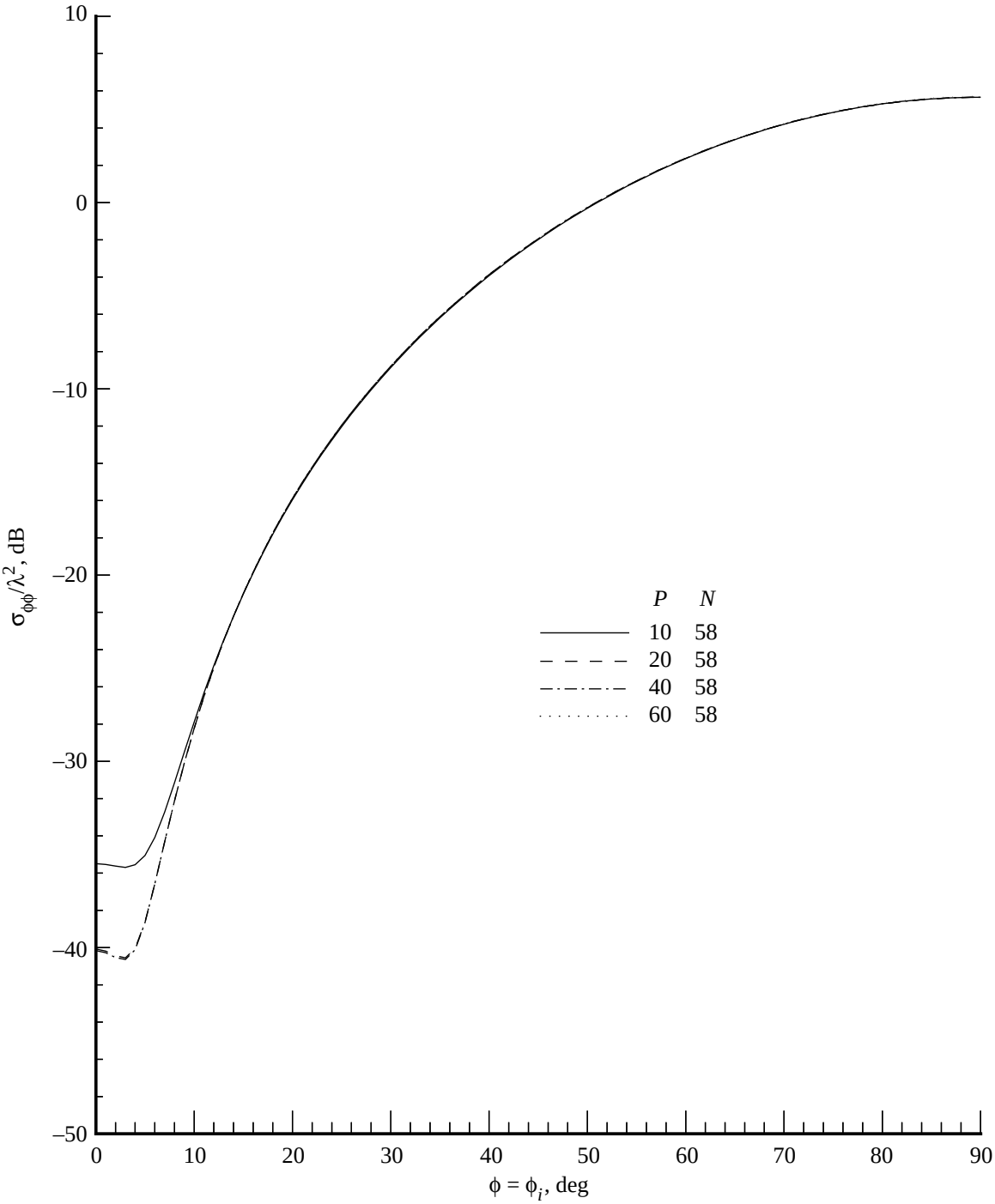

(a) E-polarization.

Figure 3. Backscatter RCS patterns for rectangular aperture backed by rectangular cavity ($a = 0.7\lambda_0$, $b = 0.1\lambda_0$, $c = 1.73\lambda_0$) recessed in an infinite ground plane ($\theta = \theta_i = 40.0°$) with $N = 58$ and $P = 10$, 20, 40, and 60.

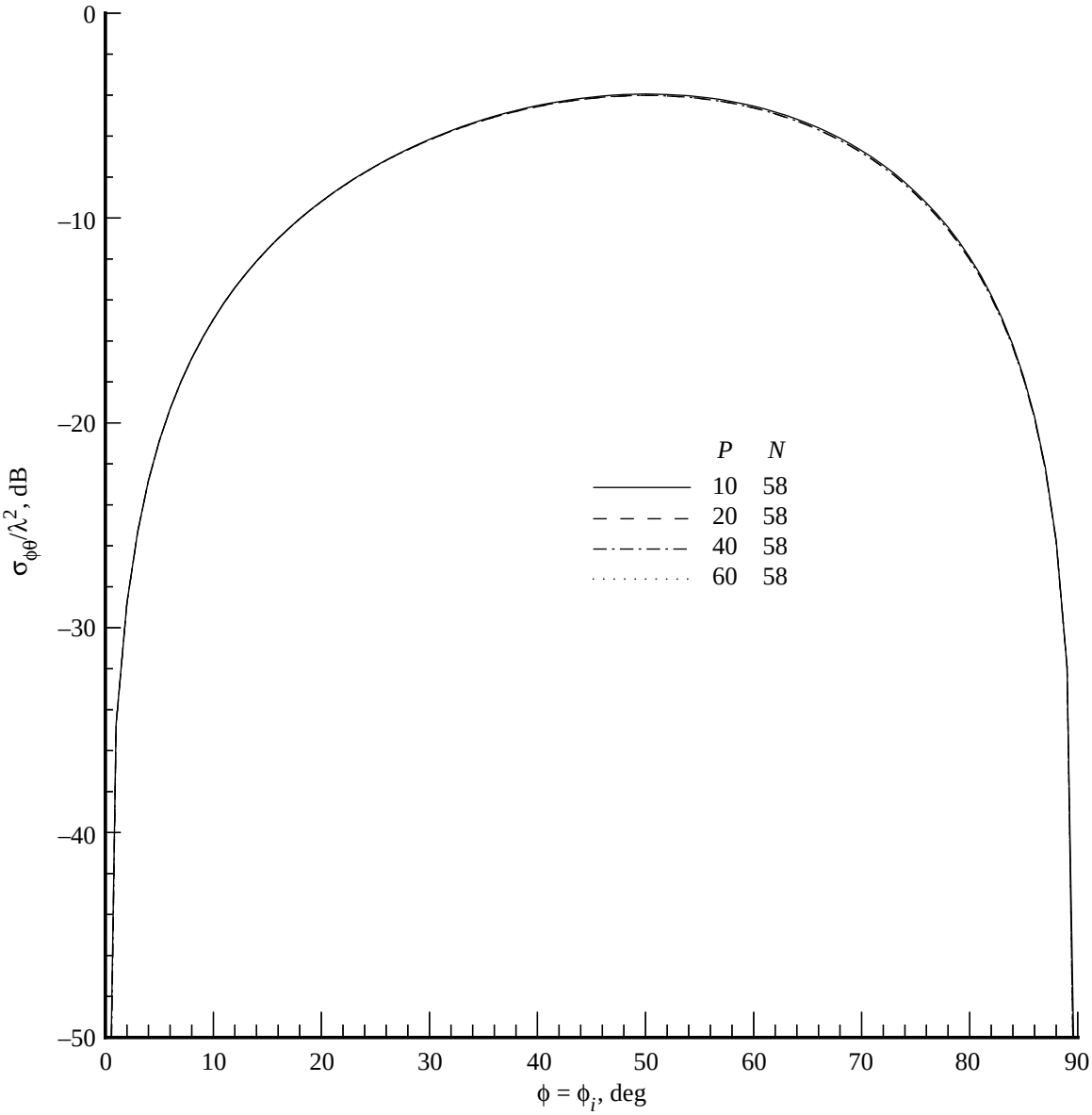

(b) Cross polarization.

Figure 3. Continued.

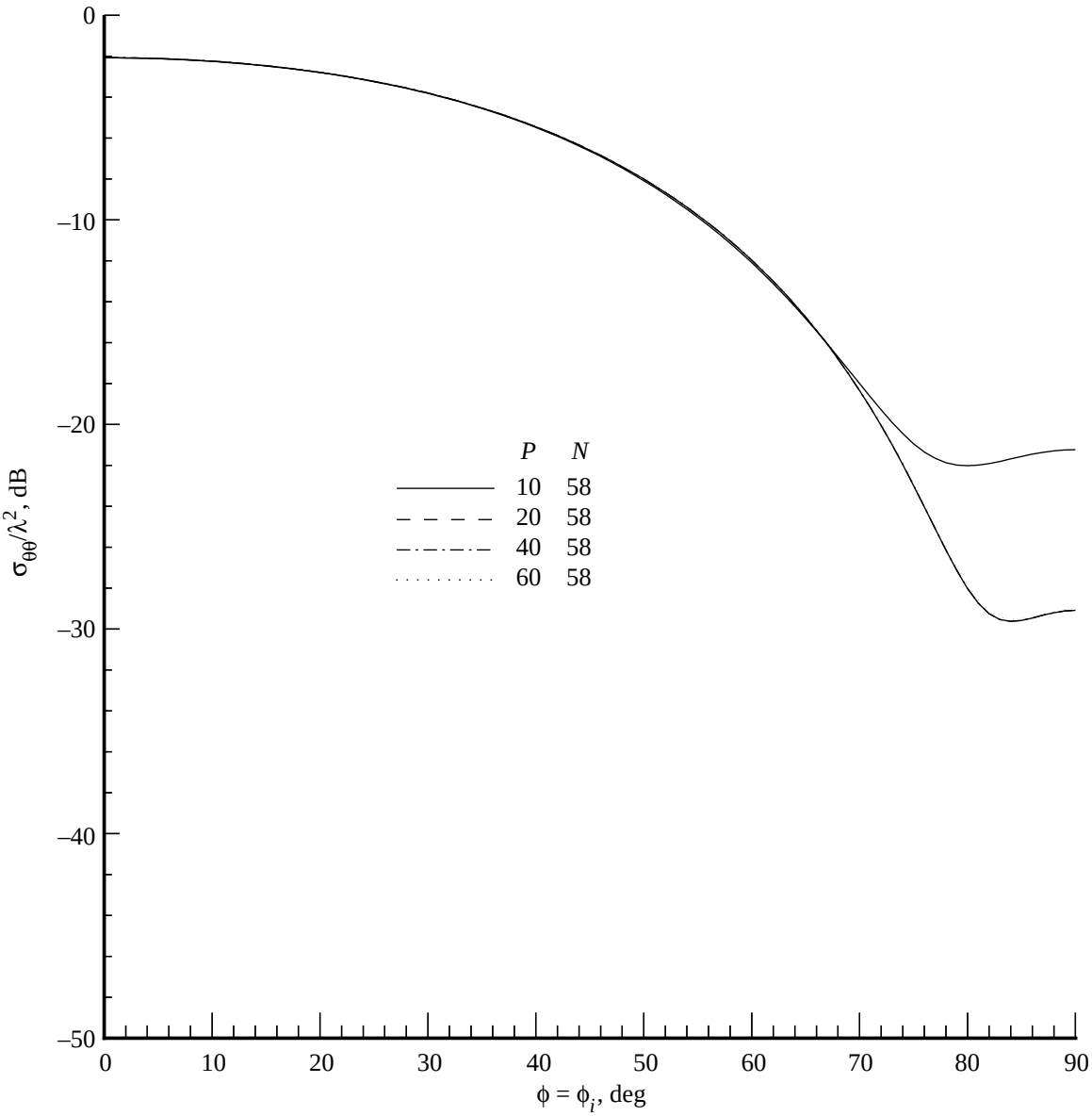

(c) H-polarization.

Figure 3. Concluded.

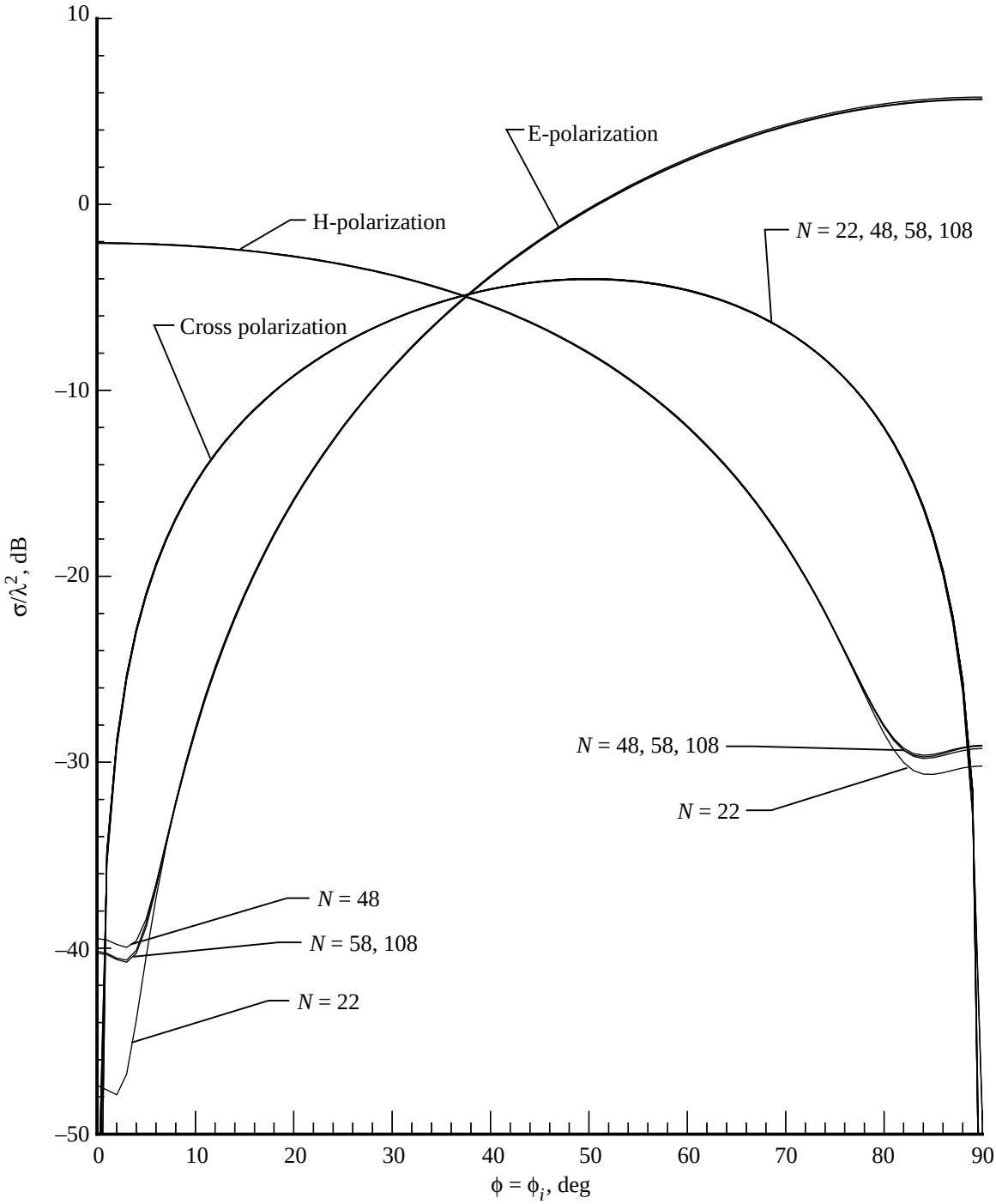

Figure 4. Backscatter RCS patterns for rectangular aperture backed by rectangular cavity ($a = 0.7\lambda_0$, $b = 0.1\lambda_0$, $c = 1.73\lambda_0$) recessed in an infinite ground plane ($\theta = \theta_i = 40.0°$) with $P = 40$ and $N = 22$, 48, 58, and 108.

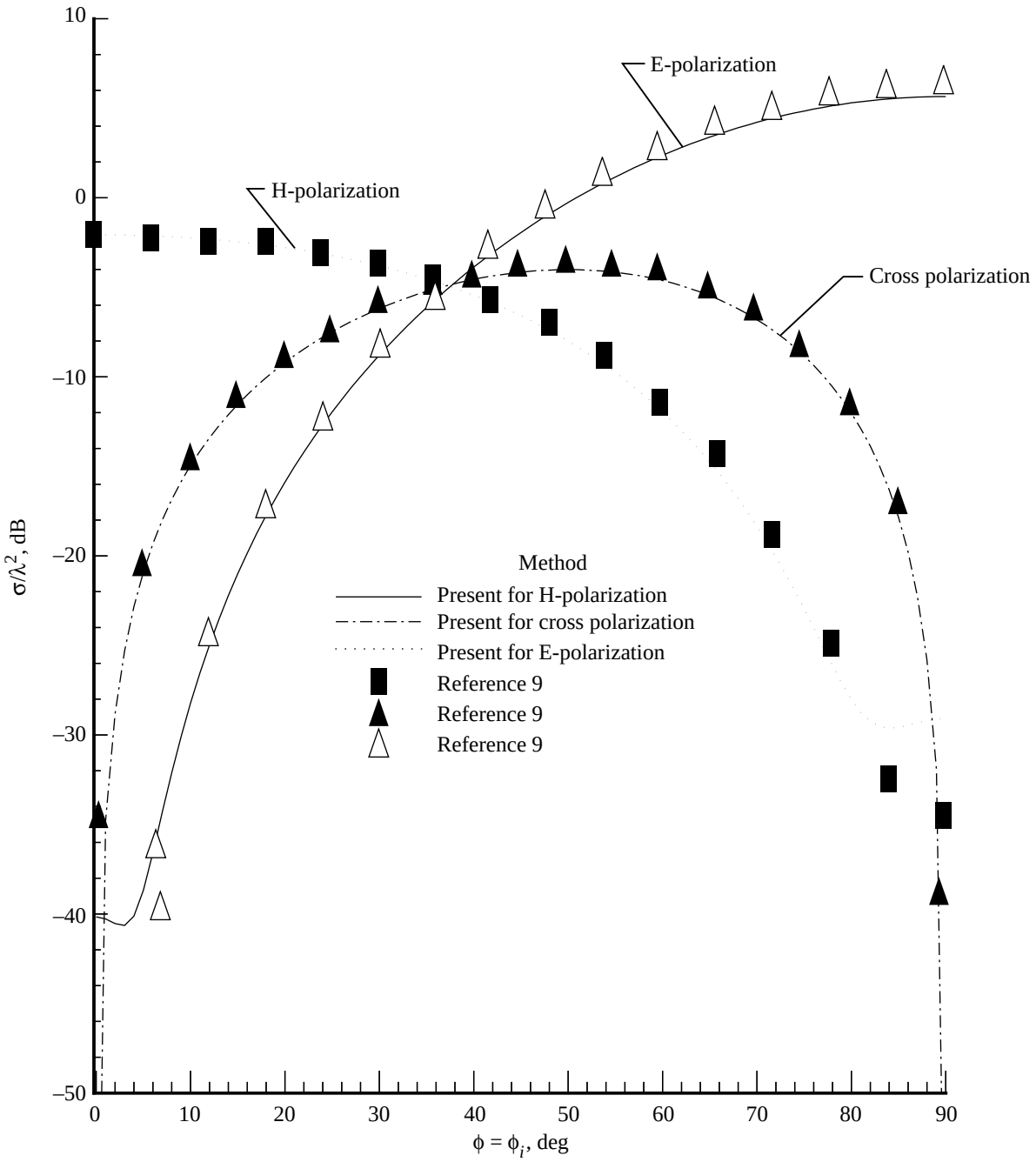

Figure 5. Backscatter RCS patterns for rectangular aperture backed by rectangular cavity ($a = 0.7\lambda_0$, $b = 0.1\lambda_0$, $c = 1.73\lambda_0$) recessed in an infinite ground plane ($\theta = \theta_i = 40.0°$) with $P = 40$ and $N = 58$ and results from reference 9.

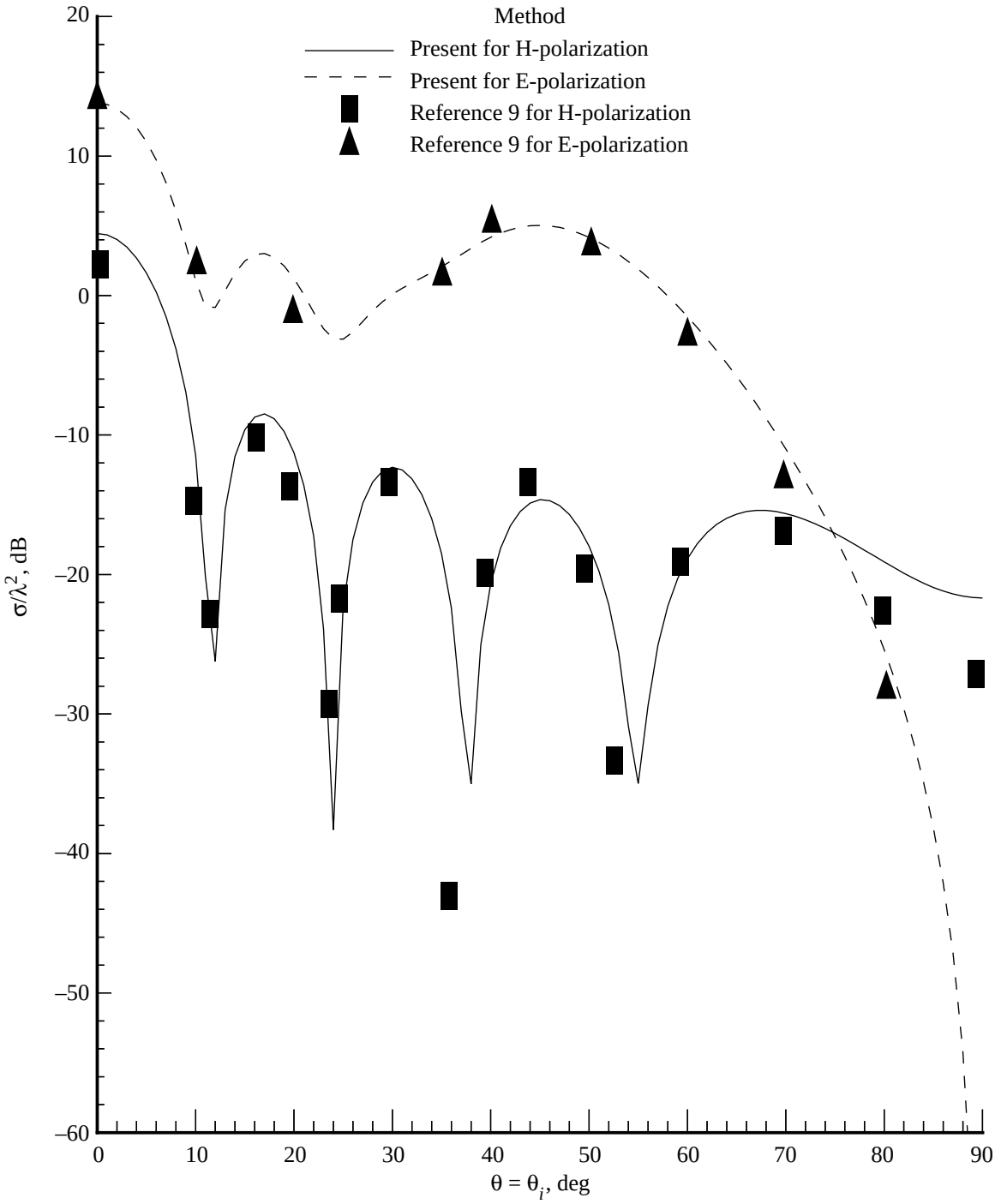

(a) $\phi = \phi_i = 0.0°$.

Figure 6. Backscatter RCS patterns for rectangular aperture backed by rectangular cavity ($a = 2.5\lambda_0$, $b = 0.25\lambda_0$, $c = 0.25\lambda_0$) recessed in an infinite ground plane with $P = 40$ and $N = 108$ and results from reference 9.

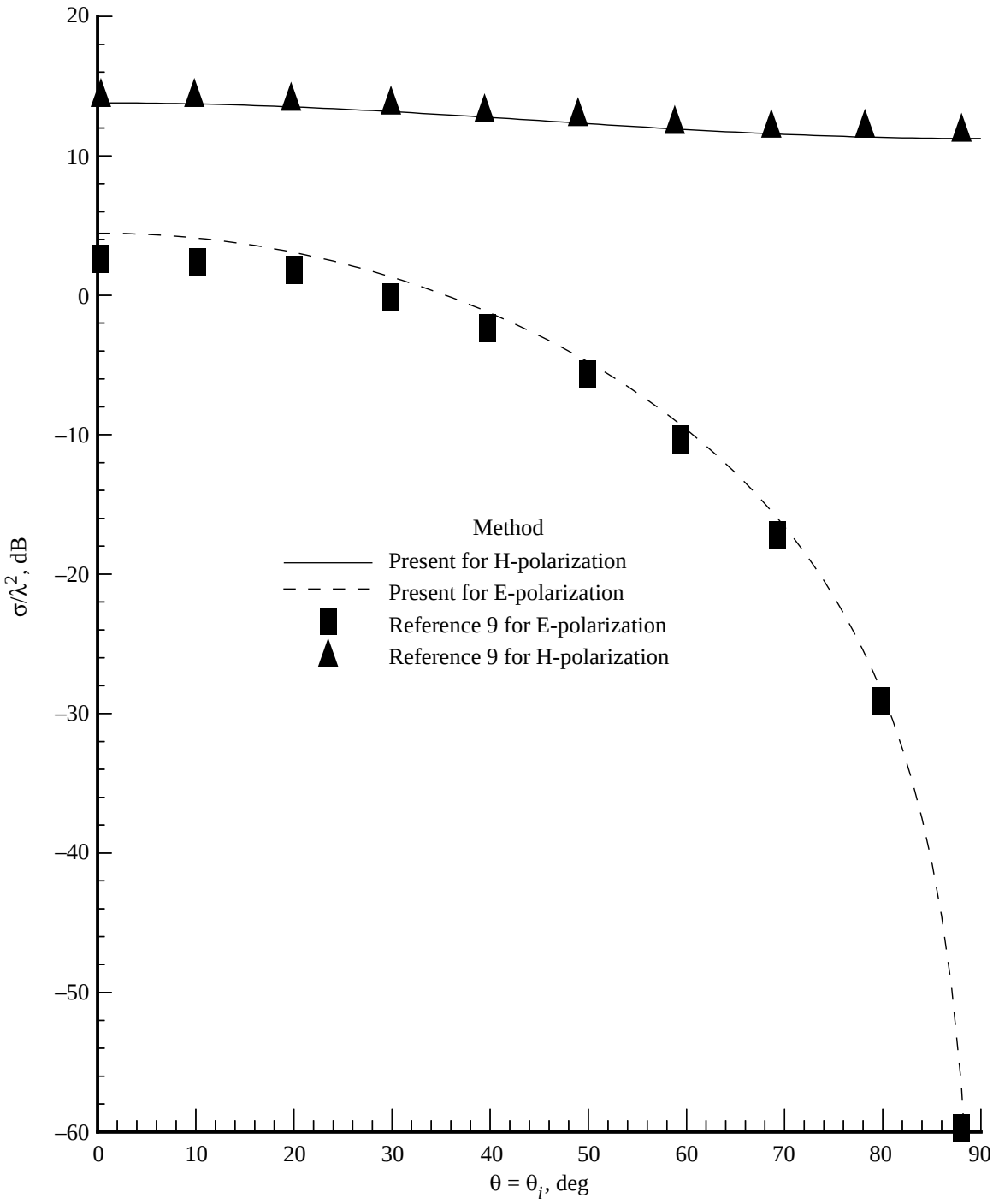

(b) $\phi = \phi_i = 90.0°$.

Figure 6. Concluded.

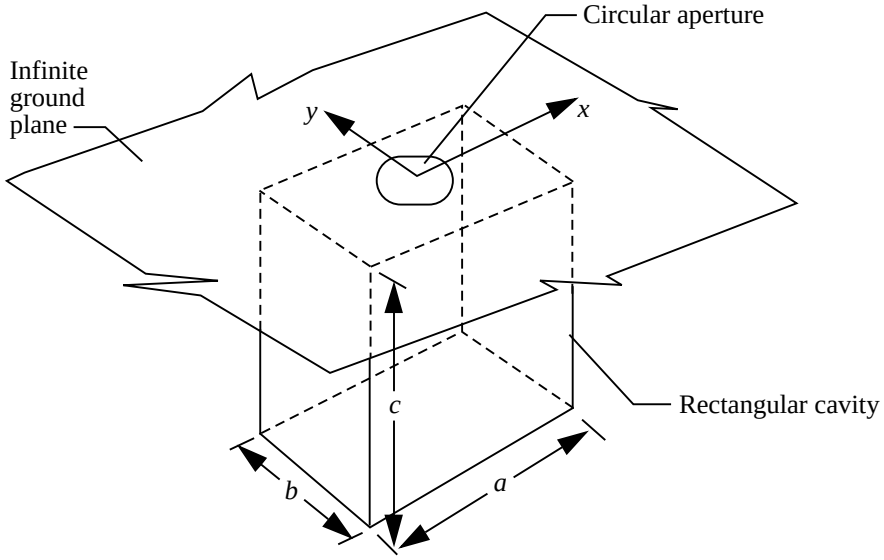

Figure 7. Geometry of circular aperture backed by rectangular waveguide.

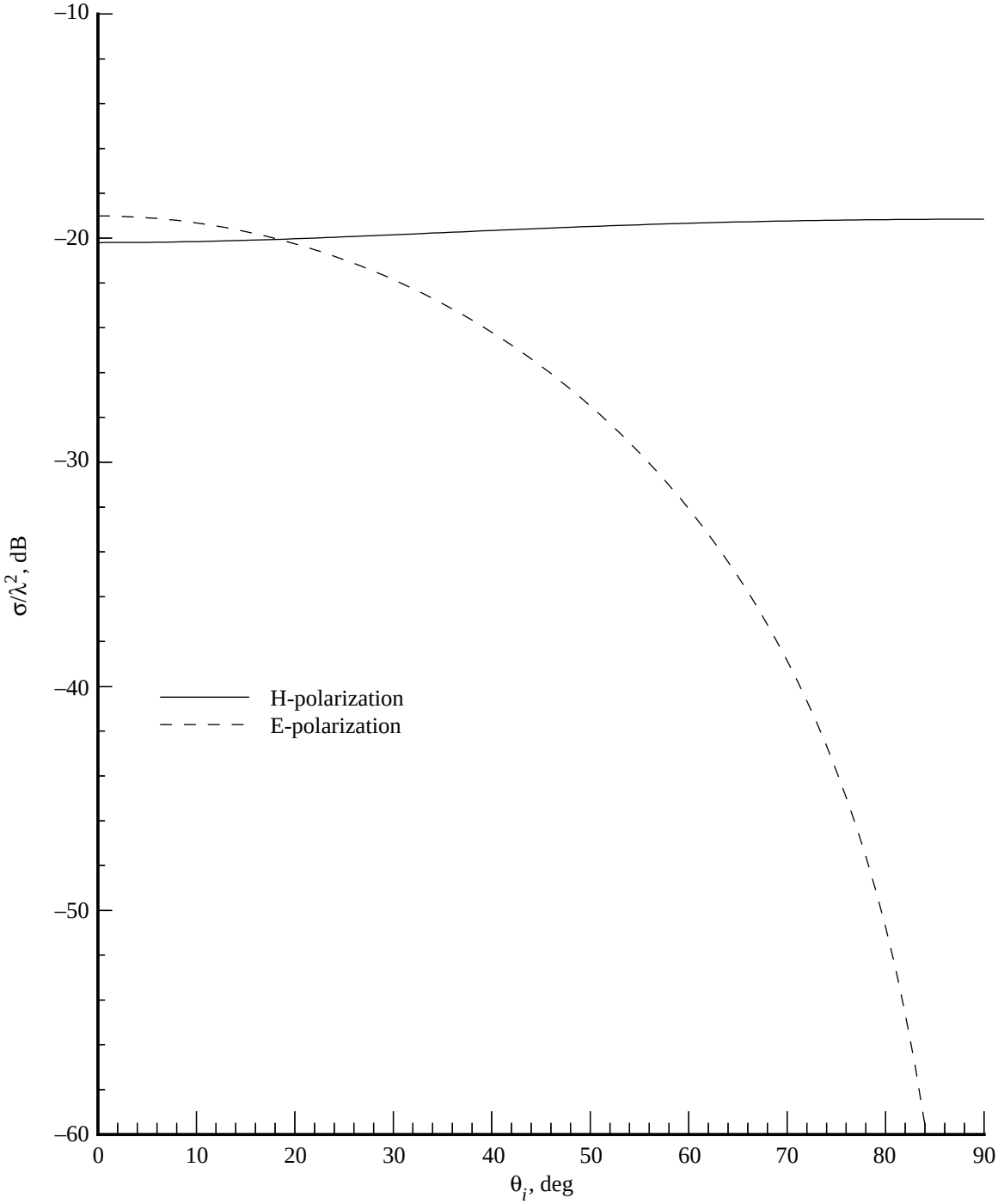

(a) $\phi = 0°$.

Figure 8. Backscatter cross section of circular aperture of radius equal to $0.11\lambda_0$ and backed by rectangular cavity as shown in figure 7 with $a = 2.5\lambda_0$, $b = 0.25\lambda_0$, and $c = 0.25\lambda_0$.

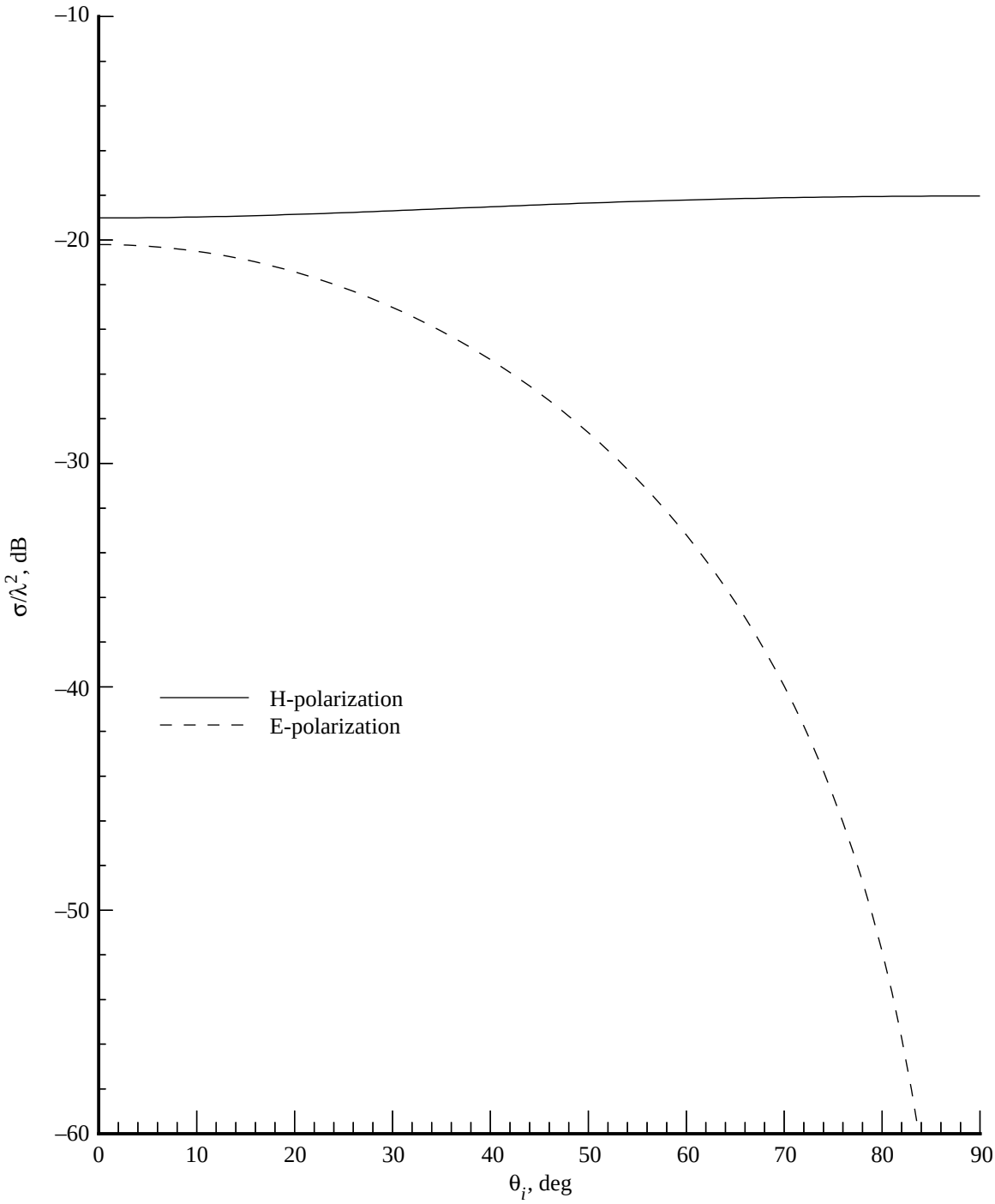

(b) $\phi = 90°$.

Figure 8. Concluded.

REPORT DOCUMENTATION PAGE

Form Approved
OMB No. 0704-0188

1. AGENCY USE ONLY *(Leave blank)*	2. REPORT DATE	3. REPORT TYPE AND DATES COVERED
	May 1997	Technical Paper

4. TITLE AND SUBTITLE
Electromagnetic Scattering From Arbitrarily Shaped Aperture Backed by Rectangular Cavity Recessed in Infinite Ground Plane

5. FUNDING NUMBERS
WU 505-64-52-04

6. AUTHOR(S)
C. R. Cockrell and Fred B. Beck

7. PERFORMING ORGANIZATION NAME(S) AND ADDRESS(ES)
NASA Langley Research Center
Hampton, VA 23681-0001

8. PERFORMING ORGANIZATION REPORT NUMBER
L-17589

9. SPONSORING/MONITORING AGENCY NAME(S) AND ADDRESS(ES)
National Aeronautics and Space Administration
Washington, DC 20546-0001

10. SPONSORING/MONITORING AGENCY REPORT NUMBER
NASA TP-3640

11. SUPPLEMENTARY NOTES

12a. DISTRIBUTION/AVAILABILITY STATEMENT
Unclassified–Unlimited
Subject Category 17
Availability: NASA CASI (301) 621-0390

12b. DISTRIBUTION CODE

13. ABSTRACT *(Maximum 200 words)*

The electromagnetic scattering from an arbitrarily shaped aperture backed by a rectangular cavity recessed in an infinite ground plane is analyzed by the integral equation approach. In this approach, the problem is split into two parts: exterior and interior. The electromagnetic fields in the exterior part are obtained from an equivalent magnetic surface current density assumed to be flowing over the aperture and backed by an infinite ground plane. The electromagnetic fields in the interior part are obtained in terms of rectangular cavity modal expansion functions. The modal amplitudes of cavity modes are determined by enforcing the continuity of the electric field across the aperture. The integral equation with the aperture magnetic current density as an unknown is obtained by enforcing the continuity of magnetic fields across the aperture. The integral equation is then solved for the magnetic current density by the method of moments. The electromagnetic scattering properties of an aperture backed by a rectangular cavity are determined from the magnetic current density. Numerical results on the backscatter radar cross-section (RCS) patterns of rectangular apertures backed by rectangular cavities are compared with earlier published results. Also numerical results on the backscatter RCS patterns of a circular aperture backed by a rectangular cavity are presented.

14. SUBJECT TERMS
Rectangular cavity backed; Radar cross section; Modal analysis

15. NUMBER OF PAGES
25

16. PRICE CODE
A03

17. SECURITY CLASSIFICATION OF REPORT	18. SECURITY CLASSIFICATION OF THIS PAGE	19. SECURITY CLASSIFICATION OF ABSTRACT	20. LIMITATION OF ABSTRACT
Unclassified	Unclassified	Unclassified	